



Review

# Current Developments in $\mu$ MAS NMR Analysis for Metabolomics

Covadonga Lucas-Torres <sup>†</sup>  and Alan Wong <sup>\*,†</sup> 

NIMBE, CEA, CNRS, Université Paris-Saclay, CEA Saclay, 91191 Gif-sur-Yvette, France; covadonga.lucas-torres-perez@cea.fr

\* Correspondence: alan.wong@cea.fr; Tel.: +33-(0)1-69-08-41-05

† These authors contributed equally to this work.

Received: 26 December 2018; Accepted: 4 February 2019; Published: 6 February 2019



**Abstract:** Analysis of microscopic specimens has emerged as a useful analytical application in metabolomics because of its capacity for characterizing a highly homogenous sample with a specific interest. The undeviating analysis helps to unfold the hidden activities in a bulk specimen and contributes to the understanding of the fundamental metabolisms in life. In NMR spectroscopy, micro( $\mu$ )-probe technology is well-established and -adopted to the microscopic level of biofluids. However, this is quite the contrary with specimens such as tissue, cell and organism. This is due to the substantial difficulty of developing a sufficient  $\mu$ -size magic-angle spinning (MAS) probe for sub-milligram specimens with the capability of high-quality data acquisition. It was not until 2012; a  $\mu$ MAS probe had emerged and shown promises to  $\mu$ g analysis; since, a continuous advancement has been made striving for the possibility of  $\mu$ MAS to be an effective NMR spectroscopic analysis. Herein, the mini-review highlights the progress of  $\mu$ MAS development—from an impossible scenario to an attainable solution—and describes a few demonstrative metabolic profiling studies. The review will also discuss the current challenges in  $\mu$ MAS NMR analysis and its potential to metabolomics.

**Keywords:** NMR; metabolomics; magic-angle spinning; HR-MAS; micro-MAS; metabolic profiling

## 1. Introduction

The study of metabolome within the organism, tissue, cell, fluid or other biomaterials can be carried out by several analytical techniques, NMR is one of the accomplished spectroscopic methods. It is capable of accurately annotating the metabolic profile with high reproducibility in a quantitative fashion. The versatility of NMR to different sampling morphologies (from liquid to semi-solid) and volume (from  $\mu$ L to nL) has significantly widened the application to metabolomics. Hence, it is utmost important that new strategies for NMR instrumentation and methodologies [1–4] must be continued striving forwards to preserve NMR spectroscopy as a frontline analytical platform in metabolomics.

NMR is intrinsically hindered by the low detection sensitivity, with an average detection of about 20–30 metabolites in the micromolar sample. As a result, NMR is often limited by the need for large sampling volume (ca. 500  $\mu$ L), obstructing the analysis of microscopic level samples. The use of high-field magnets (i.e.,  $B_0 > 16$  T) is an approach to enhance the sensitivity. However, the running cost is exponential with the field. A cost-effective method to microscopic sample is the use of miniature  $\mu$ -size detection coil for maximizing the filling factor (i.e., the sample volume close to the detection volume). The prime concern and difficulty of using  $\mu$ coil is maintaining the *high spectral resolution* data for metabolomics studies; this is generally done by matching the magnetic susceptibility of the  $\mu$ coil materials [5], or by the use of zero-susceptibility  $\mu$ coil [6]. The method of  $\mu$ coil in solution NMR has now become a routine approach to study nL samples; and it has advanced to high-throughput capability [7] with the possibility of combining with liquid chromatography in metabolomics [8] and

with advanced sorting microfluidics [9–11]. The fact that microscopic samples – organisms, tissues or cells – can be optimally detected and analyzed with a cost-effective approach makes  $\mu$ coil an extremely appealing technology for  $\mu$ NMR spectroscopy.

Despite the advancements,  $\mu$ coil in magic-angle spinning (MAS)—for complex samples like the intact organism, tissue and cell—is substantially lagging. This is due to the challenges of implementing a durable MAS stator with a  $\mu$ coil that can endure the rapid sample spinning without sacrificing the quality (both resolution and sensitivity) of data acquisition. The early designs of  $\mu$ MAS were centering the idea of implanting an additional  $\mu$ coil onto a conventional MAS probe and utilizing the existing stator to propel the sample spinning. The first  $\mu$ MAS was introduced in 2006 with a piggybacked design [12]. It consists of the  $\mu$ g-sample piggybacking on top of a standard rotor for sample spinning. Additional static  $\mu$ coil is placed around the sample for detection with an optimal filling factor. Shortly after in 2007, another approach was introduced. It utilizes the concept of inductive coil coupling [13]. A self-inductive resonator (denoted as magic-angle coil spinning (MACS)) is wrapped around the  $\mu$ g-sample and placed inside a standard rotor. Essentially, both the MACS and the  $\mu$ g-sample are spun ensemble converting a conventional MAS probe to a  $\mu$ MAS by the inductive coupling between the MAS coil and the spinning MACS  $\mu$ coil.

In 2012, JEOL Resonance Inc. introduced the first commercial standalone  $\mu$ MAS probe, in which the MAS stator consisted of a fixed 0.75-mm  $\mu$ coil (coil-diameter) [14,15]; later in 2015, Bruker launched a 0.7-mm  $\mu$ MAS probe [16]. These commercial  $\mu$ -probes are explicitly designed for ultra-fast sample spinning up to 110 kHz offering the possibility of acquiring narrow  $^1\text{H}$  NMR signals for characterizing solid materials. Since many new and exciting NMR applications have emerged in the field of material science [17] and biological science [18]. However, the optimal spectral resolution acquired from these  $\mu$ MAS probes is highly insufficient for metabolic investigations. It was not until 2012; a  $\mu$ MAS probe had emerged and demonstrated the possibility of metabolic profiling with  $\mu$ g tissues [19]. This mini-review highlights the different strategies and progress of the development of  $\mu$ MAS NMR spectroscopy towards  $\mu$ g-scale biospecimens.

#### *The Basic Criteria of $\mu$ MAS for Metabolomics*

As in most NMR-based metabolomic studies, to assure reliable dataset are acquired for the analysis, the method— $\mu$ MAS NMR in this case—must at minimal attain the following essential specification criteria:

- **Detection sensitivity:** The unequivocal identification and quantification of the metabolites are the critical aspects of metabolomics. In NMR, the adequate signal-to-noise ratio (SNR) is essential; the standardized requirement for the limit of detection (LOD) and quantification (LOQ) are  $\text{SNR} \geq 3$  and 10, respectively [20,21].
- **Spectral resolution:** Aside from the fact that high spectral resolution improves sensitivity, it also facilitates the unfolding of the dense metabolic NMR signal patterns (e.g., the 3–5 ppm range in a  $^1\text{H}$  spectrum) and allowing thorough peak analyses (identification and quantification). The acceptable  $^1\text{H}$  resolution by HR-MAS NMR is about 0.005 ppm (i.e., 2.5 Hz at 11.7 T) [22].
- **Spectral repeatability:** Metabolic profiling relies predominantly on multivariate and quantification data analysis; thus, the capability of acquiring homogenous data from the same sampling pool is crucial. This depends on the stability of the NMR instrumentation (including the probe) and also the sample preparation.
- **Sample preparation:** The precision and accuracy in the sample obtainment and sample preparation are of importance to avoid biased interpretation of the metabolic responses; therefore, a clean and reliable sample preparation must be established for all study models.

These criteria are essentially the basic guidelines for the development. In the search for a suitable  $\mu$ MAS technology, several approaches have been attempted; and among them, HR-MACS and HR- $\mu$ MAS show promising signs for metabolic investigation with a capability for acquiring good quality data for an unbiased data analysis and interpretation.

## 2. $\mu$ MAS Approaches to Metabolomics

### 2.1. $\mu$ MAS Using A Sample Configuration

Efforts have been made to analyze mass-limited samples with an improved spectral quality. The conventional methods are by: (i) applying high magnetic field acquisition with a standard volume NMR probe, or by (ii) the use of diluted NMR-observable nuclei to limit the internal spin-spin interaction. In 2013, an attempt was made using a standalone 1.6-mm MAS probe to analyze a 150  $\mu$ g skeletal muscle tissue [23] at 21.1 T (900 MHz for  $^1\text{H}$ ). To maximize the spectral quality acquisition (in both sensitivity and resolution), the  $\mu$ g biopsy is strategically placed at the center of the rotor by two susceptibility-matched Kel-F inserts (Figure 1a) for facilitating the field shimming. Moreover, the inserts also prevent from sample leakage during the rapid spinning. Indeed, the high magnetic field acquisition permits an excellent sensitivity for  $\mu$ g tissues (SNR = 37 in just 4-min acquisitions). However, as shown in Figure 1b the resolution is highly insufficient for metabolic profiling; aside from the significant lipid signals, only a few metabolites (i.e., glutamine, creatine/lysine, choline, and sugar derivatives) can be considered identifiable from the spectrum.

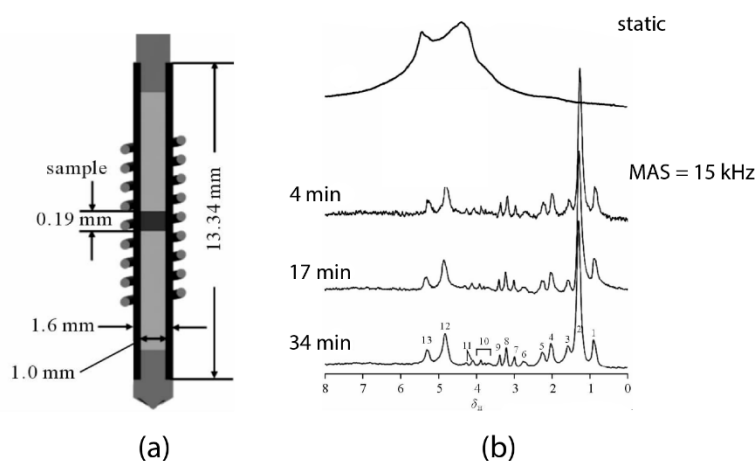


**Figure 1.** (a) The sample-configuration in a 1.6-mm rotor with Kel-F inserts [23]. (b) Spectral comparison  $^1\text{H}$  magic-angle spinning (MAS) NMR of a mouse muscular tissue at 21.1 T (900 MHz for  $^1\text{H}$ ) between non-sample spinning acquisition and spinning at 15,000 Hz with increasing acquisition time [23]. Modified with permission from the author.

This substandard resolution is ascribed to the susceptibility broadening ( $\Delta S \propto B_0 \Delta\chi_{ij} / r_{ij}^3$ ), with the presence of large magnetic susceptibility gradients ( $\Delta\chi_{ij}$ ) between the  $\mu$ g tissue and the non-spinning components of the MAS stator including the wire of the  $\mu$ coil (i.e., copper-wire). The submillimeter apart ( $r_{ij}$ ) between the sample and stator renders a substantial susceptibility broadening. Also, the study relied on a high magnetic field  $B_0$  (21.1 T) for increasing the sensitivity with a  $\mu$ g tissue, but it affiliated at the cost of susceptibility broadening that could obscure the J-splitting for metabolic identifications.

### 2.2. $\mu$ MAS Using a Spinning $\mu$ Coil: High-Resolution Magic-Angle Coil Spinning (HR-MACS)

The design of HR-MACS [24] is originated from MACS [13]. It is a straightforward approach for converting a standard MAS probe into a  $\mu$ MAS by using an inductive-coupled spinning  $\mu$ coil. Essentially, a standard size rotor contains a small sampling capillary with a wound  $\mu$ coil. The ensemble

spinning at magic-angle suppresses the susceptibility line-broadening effect ( $\Delta S \propto B_0 \Delta \chi_{ij} / r_{ij}^3$ ) ascribed from the sample, capillary, and  $\mu$ coil. The main advantage of MACS is its versatility; it can readily adapt to different NMR probes (liquid or MAS) at various fields. The teams of Wong and Nicholson have carried out an evaluation of the original MACS for metabolic profiling with 500  $\mu$ g of animal and human tissues [19] (Figure 2a). Despite the seven-fold sensitivity enhancement by MACS, the spectral resolution is visibly poor (0.1 ppm at best, or 40 Hz at 9.4 T) as compared to that obtained from HR-MAS with mg tissues; however, a few important metabolites (i.e., lipids, lactate, choline, creatine) were identified. This report had offered the first glimpse of profiling  $\mu$ g tissues by  $\mu$ MAS NMR.

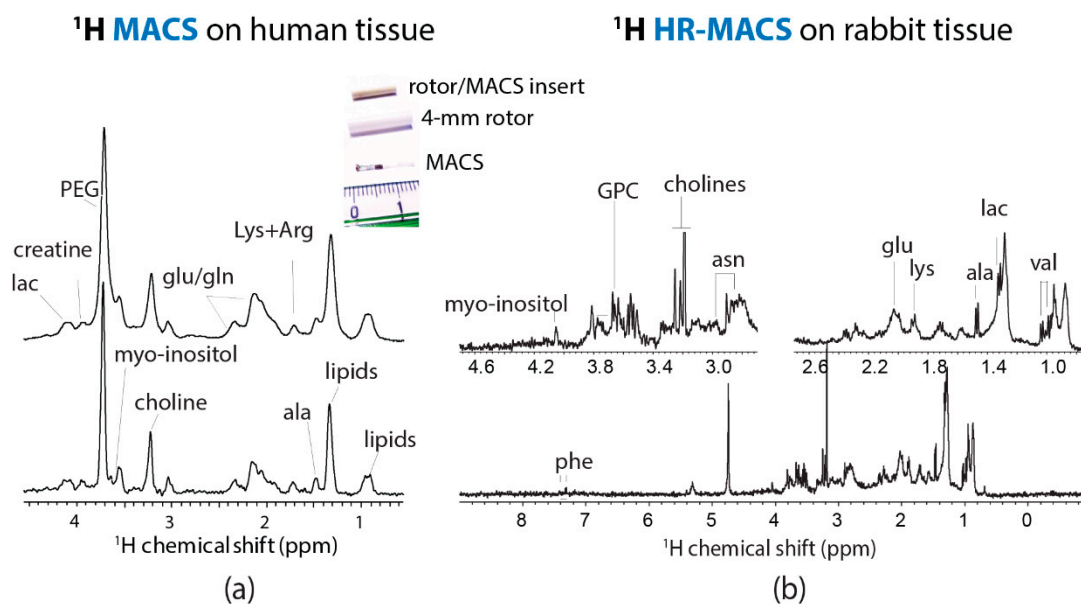


**Figure 2.** (a)  $^1\text{H}$  MACS NMR of approximately 500  $\mu$ g of human tissue at 400 MHz with MAS at 1360 Hz, with about 15 identified metabolites. Adapted with permission from [19]. Copyright (2012) American Chemical Society. (b)  $^1\text{H}$  HR-MACS NMR of 250  $\mu$ g rabbit kidney tissue at 500 MHz with MAS at 300 Hz. The improved spectral resolution offers a rich metabolic profile with about 20 identified metabolites. Adapted with permission from [24]. Copyright (2012) American Chemical Society.

Unlike the aforementioned line-broadening, the broad line width ascribed from MACS is originated from the sample temperature gradient generated by the eddy current in a spinning  $\mu$ coil, and the insuppressible (by MAS) anisotropic magnetic susceptibility of the rotor insert [24]. The design of HR-MACS is essentially a refinement of MACS by minimizing these effects to achieve high spectral quality data down to 0.02 ppm (10 Hz at 11.7 T).  $^1\text{H}$  HR-MACS NMR was first demonstrated on a 250  $\mu$ g rabbit kidney tissue biopsy (Figure 2b). The resolution has dramatically improved from 0.10 to 0.02 ppm—with the visible signature doublets of alanine and valine—while with a 6.7-fold enhancement in sensitivity. To put in a perspective of the sensitivity gain, without HR-MACS (or  $\mu$ coil in general), it would require 45 times ( $6.7^2$ ) longer in acquisition for a conventional 4-mm HR-MAS to obtain a spectral data of a 250  $\mu$ g tissue with the same SNR. The resultant quality from HR-MACS has permitted rich-metabolic profiling with a total of 25 metabolites, on par with the HR-MAS NMR from an mg-scale tissue.

Exploiting the high-quality acquisition with HR-MACS,  $^1\text{H}$  NMR-based metabolomics were performed on  $\mu$ g-samples of intact organisms. The demonstration on the intact yeast cells of *Saccharomyces cerevisiae* shows the capability of HR-MACS to comprehensively profile the metabolite constituents (with about 20 metabolites) in a 250 nL of cells, allowing to apply multivariate data analysis to precise their different conditions (Figure 3a) [25]. Another explorative study with HR-MACS was carried out with the whole  $\mu$ -sized organism of *Caenorhabditis Elegans* (*C. elegans*) [26]. The resultant  $^1\text{H}$  HR-MACS spectral resolution, impressively, demonstrated to be better than that of HR-MAS,

permitting identification of a metabolic profile with 31 metabolites from a sample with only about 12 worm individuals. This result represents the highest number of NMR-identified metabolites in a heterogeneous sample using  $\mu$ MAS. The high quality facilitates a discriminative analysis of two different strains of worms (wild-type *vs* *slcf-1* mutant) (Figure 3b). These two demonstrative studies in Figure 3 not only illustrate the high-quality spectra obtained by HR-MACS but also highlight the possibility of acquiring data with modest repeatability for the multivariate data analysis.

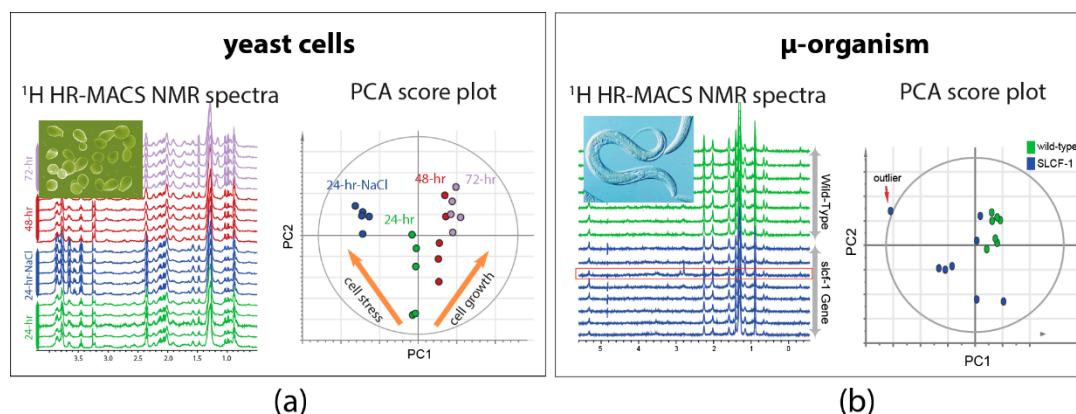


**Figure 3.**  $^1\text{H}$  HR-MACS NMR spectral comparison and the principal component analysis (PCA) of (a) different yeast cells groups and (b) different strains of *C. Elegans*. Each one of the score plot corresponding to a PCA displays the quality data validated by the explained variation ( $R^2X$ ) and the predicted variation of the models ( $Q^2$ ). In (a) the PCA (with  $R^2X(\text{sum}) = 0.793$  and  $Q^2(\text{cum}) = 0.737$ ) clearly discriminates the different cell conditions (stress and growth). Adapted with permission from [25]. Copyright (2014) Frontiers in Chemistry. In (b) the PCA (with  $R^2X(\text{sum}) = 0.964$  and  $Q^2(\text{cum}) = 0.8$ ) confirms the reliability of the discrimination between the wild-type *C. Elegans* (green) and the strain of *slcf-1* mutant (blue) with only 12 individuals. Adapted with permission from [26]. Copyright American Chemical Society.

Pushing the detection limit, HR-MACS has successfully detected metabolite signals from a single individual of *C. elegans* with the aid of a high magnetic field (18.8 T, 800 MHz for  $^1\text{H}$ ) [26]. Although the resultant spectrum is inadequate for characterizing the metabolic activities due to the long acquisitions period (10 + h) and the presence of a substantial susceptibility broadening ( $\Delta S \propto B_0$ ), this result represents the first, and only,  $^1\text{H}$  MAS NMR detection of a single intact submillimeter organism.

One major flaw of HR-MACS is the  $\mu$ coil itself: the strenuous process in fabrication and the fragility of the  $\mu$ coil. Currently, the most effective approach for assembling an HR-MACS  $\mu$ coil is by manually-winding, which is a labour-intensive process; the degradation of the NMR performance from the  $\mu$ coil is inevitable due to the continuous centrifugation pressure exerted upon the  $\mu$ coil. Therefore, with luck prevail the current-state of HR-MACS can only be applied to study with a small number of sampling.

Several reports have acknowledged the difficulty in  $\mu$ coil fabrication. A new design on-chip MACS [27] was introduced for adopting an automated fabrication with a robotic wirebonding technology. It enables rapid manufacturing of over 100 on-chip MACS in a single procedure; however, the reported spectral resolution was rather poor with about 1 ppm (500 Hz at 11.7 T) in line width. Another MACS design (monolithic MACS) was later introduced based on a 2D-printing technology [28]. Although the manufacturing efficiency was inferior to wirebonding, it offered a better spectral quality with a line width of 0.1 ppm (50 Hz at 11.7 T).

### 2.3. A Standalone High-Resolution $\mu$ MAS Probe (HR- $\mu$ MAS)

In 2015, a standalone high-resolution capable  $\mu$ MAS probe (denoted as HR- $\mu$ MAS) was introduced [29]. It has the capacity of acquiring high-quality data from a 500 nL sample, about a 50-fold smaller than that from a conventional HR-MAS (Figure 4a). It was achieved by an extensive modification on a standard 1-mm  $\mu$ MAS probe by minimizing the susceptibility gradient ( $\Delta\chi_{ij}$ ). Practically, the material of the MAS stator and the coil-wire were replaced with susceptibility-matched materials. The resultant resolution from HR- $\mu$ MAS offers a ten-fold improvement with 0.01 ppm (5 Hz at 11.7 T) (as compared to that in Figure 1b). Unlike the previous HR-MACS design, HR- $\mu$ MAS is a robust probe with a secured  $\mu$ coil offering the possibility of large-scale studies (i.e., large sampling-replicates). Moreover, homo- and hetero-nuclear correlation experiments are feasible with HR- $\mu$ MAS and have been demonstrated on  $^1\text{H}$ - $^1\text{H}$  TOCSY and  $^1\text{H}$ - $^{13}\text{C}$  HMQC experiments [29]. However, one must be cautious with the detection sensitivity.

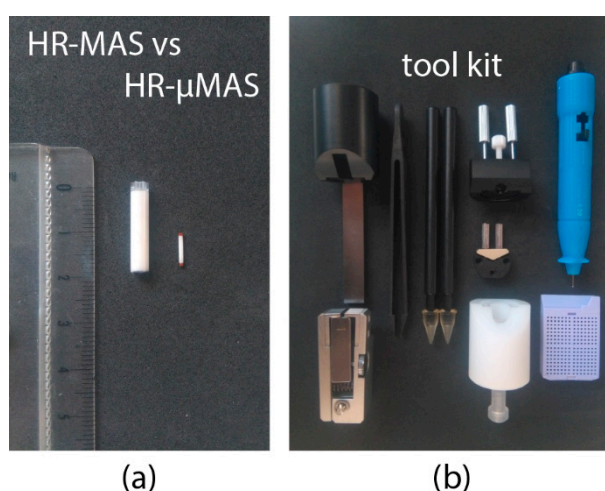


**Figure 4.** (a) MAS rotor comparison between 4-mm HR-MAS and 1-mm HR- $\mu$ MAS. (b) A typical toolkit for the sample-preparation of an HR- $\mu$ MAS experiment.

Capitalizing the merits of HR- $\mu$ MAS, HR- $\mu$ MAS NMR was successfully applied to comprehensive metabolic profiling of a food tissue [30]. Figure 5a shows the sampling of  $\mu\text{g}$  tissues with good spectral quality data (15-min acquisition with 0.03 ppm resolution), permitting localized profiling of the different anatomical regions of a garlic clove: skin, flesh, core-sprout and core-inner epidermis. More impressively, it was capable of carrying out a discriminative analysis between the two tiny regions (core-sprout and core-inner epidermis) owing to the  $\mu\text{g}$ -sampling by HR- $\mu$ MAS (Figure 5b). This is impractical with HR-MAS because of the necessity of mg-sampling, highlighting the values of  $\mu$ MAS. Essentially, this study with HR- $\mu$ MAS offers a firsthand account of  $\mu$ MAS to  $\mu\text{g}$ -analysis.

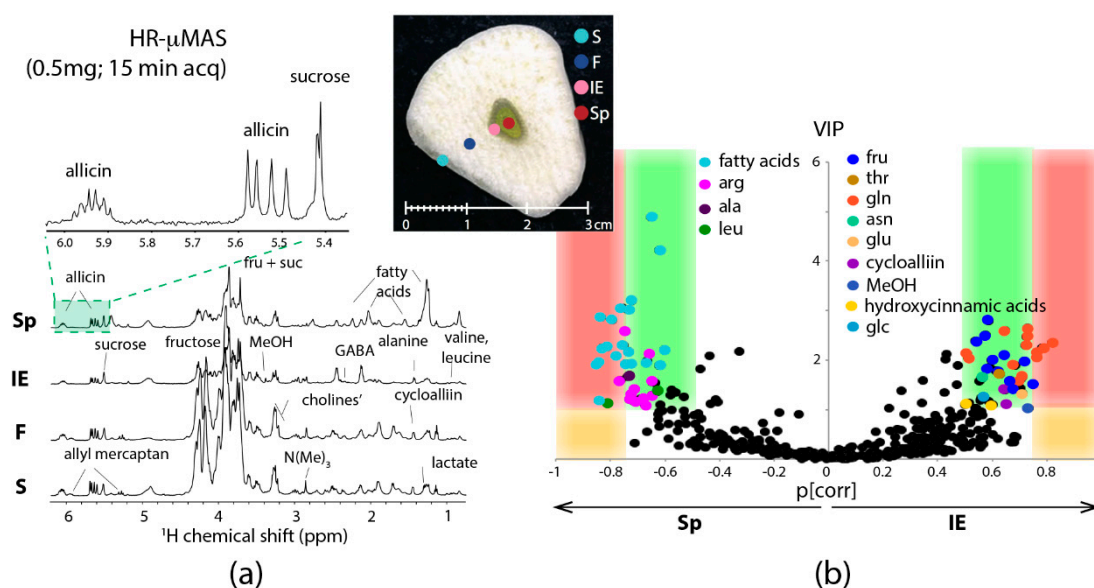


**Figure 5.** (a)  $^1\text{H}$  HR- $\mu\text{MAS}$  NMR spectra of the four regions of a garlic clove tissue at 500 MHz spinning at 4000 Hz. The inserted photo displays the four different anatomical regions: S skin, F flesh, IE inner epidermis and Sp sprout. (b) A plot comparing the two quality indicators for each variable (variable = chemical shift identified as a determined metabolite) from a discriminant analysis (OPLS-DA): the variable importance in the projection (VIP) vs the variable reliability in the model ( $p[\text{corr}]$ ). The separation between the two small regions (Sp = sprout; IE = inner epidermis) within the core of a single garlic clove is evident. With OPLS-DA quality-parameters: 1 predictive component and 1 orthogonal component,  $R^2\text{X} = 0.747$ ,  $R^2\text{Y} = 0.955$ ,  $Q^2 = 0.828$ , and a p-value of the cross-validation = 0.027. Adapted with permission from [30]. Copyright (2018) American Chemical Society.

### 3. Challenges in $\mu\text{MAS}$

#### 3.1. Sample-Preparation

Sample-preparation is a critical component in virtually all bioanalytical methods for acquiring representable data concerning the interest. Standardized experimental protocols are necessary and have been established in most NMR-based applications [22,31,32] to metabolomics. However, owing to the infancy of the  $\mu\text{MAS}$  development, currently, no robust protocols have been established. Sample-preparation may seem trivial at first glance, but it is, in fact, a demanding task for handling specimens—especially with semi-solids—at a microscopic level. One must consider the entire procedure clean and quick for preserving for the metabolic integrity. Envision the following procedure: (i) a rapid sample-extraction using a fine-needle syringe; (ii) a direct sample-filling into a  $\mu$ -size rotor and followed by (iii) a quick rotor sealing. All these steps must be handled with dedicated tools (for example Figure 4b) under a stereoscope. Moreover, one of the many complications is that the specimens should be under a cold (or favorable) temperature during the procedure.

Acknowledging the difficulty, capillary-sampling has been proposed for HR-MACS [25,26] and HR- $\mu\text{MAS}$  [33]. This permits the preparation away from the rotor, facilitating the sample-filling by simple capillary-suction for the solution or capillary-punch for the tissue. However, the drawback is the loss of detection sensitivity with a reduced filling factor. Disposable  $\mu$ -rotor (made of Kel-F) has also been considered for HR- $\mu\text{MAS}$  [29]. Similar to that of the bio-insert with HR-MAS, it allows a mass preparation, but the fragility of the Kel-F rotor has hindered a rapid preparation.

The necessity of using a rotor for sample spinning requires a sample-filling step in the preparation, which can be time-consuming and damaging to the sample. Currently, the most efficient methods are the use of micro-pipette for the solution and micro-sampling punch for tissue and occasionally abet with gentle centrifugation. The average time requires about 10–20 min for tissues; and the more

challenging specimens are cells and small organisms. Indeed, improvement is necessary. This may require new devices, such as microfluidic, for easing the sample-filling; or even an entirely new design of the  $\mu$ MAS probe that can facilitate the entire preparation. For example, a probe (or stator) that can accommodate a spinning  $\mu$ -needle,  $\mu$ -punch tip or  $\mu$ -pipette tip without the need of a sample rotor. This would indeed eliminate the strenuous task of sample filling.

### 3.2. Detection Sensitivity

Although  $\mu$ coil improves the mass-sensitivity (i.e., SNR per unit mass) of microscopic samples to its maximum capacity, the overall sensitivity is still intrinsically inferior as compared to that of a large-mass detection – if available – with the standard HR-MAS. As an example, the sensitivity (in SNR per unit acquisition period) from HR-MACS with 12 *C. elegans* worm population is nearly 200-fold less than that of HR-MAS with a population of 1000+ [26]. This indeed limits the capacity in the analysis.

It is well-established that data acquisition at high magnetic field enhances the sensitivity ( $\text{SNR} \propto B_0^{3/2}$ ) (e.g., the use of 21.1 T for profiling a  $\mu\text{g}$ -tissue [23] and a single-organism [26]), but at a cost of increasing the susceptibility gradient effect ( $\Delta S \propto B_0$ ), and may lead to uncorrectable (i.e., by shimming) line-broadening. Increasing the signal-averaging could also enhance the sensitivity ( $\text{SNR} \propto \sqrt{\text{scan}}$ ); however, it demands a considerable acquisition period that could contribute to sample degradation. Therefore, designing a  $\mu$ MAS study should be made with caution.

### 3.3. High-Throughput Analysis

The capability of high-throughput analysis—with the help of automated sampling and data acquisitions—has made NMR spectroscopy an efficient analytical tool in metabolomics. The challenge with  $\mu$ MAS is the limitation in sample-preparation and detection sensitivity described above. Each factor requires an extensive time as compared to the conventional HR-MAS: 10–20 minutes for sample-preparation and another 30–120 min for data acquisition. Indeed, these are the bottlenecks of  $\mu$ MAS to metabolomics and have prevented from the high-throughput analysis.

## 4. But Why $\mu$ MAS?

A prime advantage of analyzing a microscopic specimen is the high level of homogeneity in the sample. This allows a candid characterization of the interest metabolic responses and helps to unfold the complexity of the biological variability. On the contrary, this information often conceals or is lost in the analysis of bulk size sample because of its high heterogeneity. Often it requires complex chemometric schemes for extracting the relevant information. One beneficial factor of  $\mu$ MAS is the invasiveness nature on the specimen with a minimal sample-manipulation.

In clinical science, microscopic sample analysis—as a complementary approach to advanced imaging techniques—could enhance the sensitivity of recognizing the modified metabolic patterns of the disease in tissue and may improve on the prognosis, diagnosis and screening. The possibility of firsthand monitoring of the perturbations in metabolic responses of the diseases could offer an effective and immediate personalized treatment. Moreover, since tissue excision (in the order of few mg) is currently a common practice in medicine for mg tissue analysis and is considered a non-invasive approach; with  $\mu$ MAS a sub-mg analysis could benefit the process by not only minimizing the invasiveness with  $\mu\text{g}$  excision (i.e., a signification factor for examining tissue such as human infants); but it could also reduce the necessity of large-scale surgical procedure.

In health science, the homogeneous data analysis by the microscopic-level investigation (i.e., sampling the uniform cellular tissue) could elevate the identification of the significant biomarkers of abnormality such as cancer in general [34], Alzheimer [35], and diabetes or other metabolic syndromes [36]. For example, in neuroscience, profiling the isolated neuron and astrocyte cells may help to reveal detailed insights into the fundamental of the intercellular metabolic cooperation between neurons and astrocytes for furthering in the understanding of brain metabolism [37].



In biological and ecological science, like in health science, to be able to analyze a single organism or unicellular organisms could simplify the annotation of the metabolic variant associated to the biological variability and differential susceptibility of the environment. On this basis, one could investigate the long-term harmful effects of pollutants on endangered species [38,39] by monitoring the changes in the metabolism of a single mosquito larvae due to pesticides [40], or a single amphipod for the exposure to toxic marine sediments [41]. These examples could benefit from  $\mu$ MAS microscopic analysis because of the non-destructive nature of the experiment, especially with small-sample diameter, which diminishes the centrifugation force exerted on a spinning sample.

In agricultural science, the analysis with  $\mu$ g samples could provide direct insights into the integration and regulation of plant metabolism: from a single seed to a grown plant. For examples, the germination process in a seed is complex and of great importance for the development of the plant seeds to form a new individual. To be able to characterize the metabolic coordination of the distinct  $\mu$ -regions in a seed could help the development of germination [42] and essentially the plant growth. This could benefit from a spatiotemporal  $\mu$ MAS NMR analysis on a single seed.

A spatiotemporal  $\mu$ MAS analysis could also benefit to plant research. Environmentally adverse conditions such as changes in soil salinity [43] or water scarcity [44] are adverse circumstances that affect directly to plant roots and, consequently, to plant growth. Understanding the metabolic response to such events in localized regions of a root may elucidate the tolerant mechanisms in plants.

Similarly, in food science, fruits and vegetables in particular, could benefit from the homogeneity in sampling by  $\mu$ MAS, by supporting in the precise detection of bioactive compounds within different regions [45–47]. Thus, the microscopic-level analysis can be used to follow fruit conditions, such as the ripening process—for obtaining the optimal content of beneficial components.

## 5. Concluding Remarks

Since the first report of a  $\mu$ MAS NMR profiling in 2012, substantial advancements on  $\mu$ MAS methodology have been made, offering glimpses of a future potential NMR analysis of  $\mu$ g-scaled specimens to metabolomics. One example is the concept of clinical NMR spectroscopy proposed by Jeremy K. Nicholson and his team in 2011 [48]; however, a major hindrance is the analysis of mg tissue by HR-MAS. It gives highly heterogeneous information preventing an instantaneous identification of biomarkers. On the contrary, the homogeneous data from a  $\mu$ MAS analysis could offer a prompt feedback to the medical staffs for their diagnosis and prognosis.

Despite the advancement, there is no question that further improvements in detection sensitivity and sample-preparation are necessary to unlock the bottlenecks of  $\mu$ MAS analysis, and may render the possibility of clinical NMR spectroscopy. We are convinced that one-day  $\mu$ MAS NMR analysis would become a vital component in -omics research, but it would take a collaborative effort among the different disciplines with complementary expertise to develop a reliable  $\mu$ MAS NMR methodology for high-quality data acquisition with high-throughput analysis.

**Author Contributions:** C.L.T. planned and drafted the manuscript; A.W. assisted in editing and reviewing.

**Funding:** The manuscript and APC were funded by Agence Nationale de la Recherche in France, grant numbers ANR-16-CE11-0023.

**Acknowledgments:** We would like to thank the support from JEOL Resonance Inc. for development of HR- $\mu$ MAS probe. We are also grateful to Dr Yusuke Nishiyama (JEOL) for reviewing the manuscript.

**Conflicts of Interest:** The authors declare no conflict of interest.

## References

1. Pontes, J.G.M.; Brasil, A.J.M.; Cruz, G.C.F.; de Souza, R.N.; Tasic, L. NMR-based metabolomics strategies: Plants, animals and humans. *Anal. Methods* **2017**, *9*, 1078–1096. [[CrossRef](#)]
2. Bingol, K.; Brüsweiler, R. Multidimensional Approaches to NMR-based metabolomics. *Anal. Chem.* **2014**, *86*, 47–57. [[CrossRef](#)] [[PubMed](#)]

3. Nagana Gowda, G.A.; Raftery, D. Recent advances in NMR-based metabolomics. *Anal. Chem.* **2017**, *89*, 490–510. [[CrossRef](#)] [[PubMed](#)]
4. Zalesskiy, S.S.; Danieli, E.; Blümich, B.; Ananikov, V.P. Miniaturization of NMR systems: Desktop spectrometers, microcoil spectroscopy, and “NMR on a Chip” for chemistry, biochemistry, and industry. *Chem. Rev.* **2014**, *114*, 5641–5694. [[CrossRef](#)] [[PubMed](#)]
5. Olson, D.L.; Peck, T.L.; Webb, A.G.; Magin, R.L.; Sweedler, J.V. High-resolution microcoil <sup>1</sup>H NMR for mass-limited, nanoliter-volume samples. *Science* **1995**, *270*, 1967–1970. [[CrossRef](#)]
6. Kc, R.; Henry, I.D.; Park, G.H.J.; Raftery, D. New solenoidal microcoil NMR probe using zero-susceptibility. *Concepts Magn. Reson. Part B Magn. Reson. Eng.* **2010**, *17*, 13–19. [[CrossRef](#)] [[PubMed](#)]
7. Grimes, J.H.; O’Connell, T.M. The application of micro-coil NMR probe technology to metabolomics of urine and serum. *J. Biomol. NMR* **2011**, *49*, 297–305. [[CrossRef](#)]
8. Albert, K. *LC ± NMR: Theory and Experiment*; John Wiley & Sons: Chichester, England, 2002; pp. 1–22. Available online: <https://onlinelibrary.wiley.com/doi/book/10.1002/0470854820> (accessed on 3 December 2018).
9. Lee, H.; Yoon, T.-J.; Figueiredo, J.-L.; Swirski, F.K.; Weissleder, R. Rapid detection and profiling of cancer cells in fine-needle aspirates. *Proc. Natl. Acad. Sci.* **2009**, *106*, 12459–12464. [[CrossRef](#)]
10. Bakhtina, N.A.; MacKinnon, N.; Korvink, J.G. Advanced Microfluidic assays for *Caenorhabditis elegans*. In *Advances in microfluidics—New Applications in Biology, Energy and Materials Sciences*; Intechopen: London, UK, 2016; pp. 91–114. ISBN 9789537619992. Available online: <https://www.intechopen.com/books/advances-in-microfluidics-new-applications-in-biology-energy-and-materials-sciences/advanced-microfluidic-assays-for-caenorhabditis-elegans> (accessed on 3 December 2018).
11. Spengler, N.; Höfflin, J.; Moazenzadeh, A.; Mager, D.; MacKinnon, N.; Badilita, V.; Wallrabe, U.; Korvink, J.G. Heteronuclear micro-helmholtz coil facilitates μm-range spatial and sub-Hz spectral resolution NMR of nL-volume samples on customisable microfluidic chips. *PLoS ONE* **2016**, *11*, e0146384. [[CrossRef](#)]
12. Janssen, H.; Brinkmann, A.; Van Eck, E.R.H. Microcoil high-resolution magic angle spinning NMR spectroscopy. *J. Am. Chem. Soc.* **2006**, *128*, 8722–8723. [[CrossRef](#)]
13. Sakellariou, D.; Le Goff, G.; Jacquinet, J.-F. High-resolution, high-sensitivity NMR of nanolitre anisotropic samples by coil spinning. *Nature* **2007**, *447*, 694–697. [[CrossRef](#)] [[PubMed](#)]
14. Nishiyama, Y.; Endo, Y.; Nemoto, T.; Utsumi, H.; Yamauchi, K.; Hioka, K.; Asakura, T. Very fast magic angle spinning <sup>1</sup>H-<sup>14</sup>N 2D solid-state NMR: Sub-micro-liter sample data collection in a few minutes. *J. Magn. Reson.* **2011**, *208*, 44–48. [[CrossRef](#)] [[PubMed](#)]
15. JEOL Resonance Inc. Released a 0.75-mm μMAS probe. In Proceedings of the 53rd Experimental Nuclear Magnetic Resonance Conference (ENC), Miami, FL, USA, 15–20 April 2012.
16. Bruker. Released Magic Angle spinning above 100 kHz. In Proceedings of the 56th Experimental Nuclear Magnetic Resonance Conference (ENC), Pacific Grove, CA, USA, 19–24 April 2015.
17. Deschamps, M. *Ultrafast Magic Angle Spinning Nuclear Magnetic Resonance*; Annual Reports on NMR, Academic Press, Elsevier Ltd.: Oxford, UK, 2014; pp. 109–144. ISBN 9780128001851.
18. Agarwal, V.; Penzel, S.; Szekely, K.; Cadalbert, R.; Testori, E.; Oss, A.; Past, J.; Samoson, A.; Ernst, M.; Bockmann, A.; et al. De Novo 3D Structure Determination from Sub-milligram Protein Samples by Solid-State 100 kHz MAS NMR Spectroscopy. *Angew. Chemie-Int. Ed.* **2014**, *53*, 1–5. [[CrossRef](#)] [[PubMed](#)]
19. Wong, A.; Jiménez, B.; Li, X.; Holmes, E.; Nicholson, J.K.; Lindon, J.C.; Sakellariou, D. Evaluation of high resolution magic-angle coil spinning NMR spectroscopy for metabolic profiling of nanoliter tissue biopsies. *Anal. Chem.* **2012**, *84*, 3843–3848. [[CrossRef](#)] [[PubMed](#)]
20. Shrivastava, A.; Gupta, V.B. Methods for the determination of limit of detection and limit of quantitation of the analytical methods. *Chron. Young Sci.* **2011**, *2*, 21–25. [[CrossRef](#)]
21. Lacey, M.E.; Subramanian, R.; Olson, D.L.; Webb, A.G.; Sweedler, J.V. High-Resolution NMR Spectroscopy of Sample Volumes from 1 nL to 10 μL. *Chem. Rev.* **1999**, *99*, 3133–3152. [[CrossRef](#)] [[PubMed](#)]
22. Beckonert, O.; Coen, M.; Keun, H.C.; Wang, Y.; Ebbels, T.M.D.; Holmes, E.; Lindon, J.C.; Nicholson, J.K. High-resolution magic-angle-spinning NMR spectroscopy for metabolic profiling of intact tissues. *Nat. Protoc.* **2010**, *5*, 1019–1032. [[CrossRef](#)] [[PubMed](#)]
23. Feng, J.; Hu, J.; Burton, S.D.; Hoyt, D.W. High Resolution Magic Angle Spinning <sup>1</sup>H NMR metabolic profiling of nanoliter biological tissues at high magnetic field. *Chinese J. Magn. Reson.* **2013**, *30*, 1–11.
24. Wong, A.; Li, X.; Sakellariou, D. Refined magic-angle coil spinning resonator for nanoliter NMR spectroscopy: Enhanced spectral resolution. *Anal. Chem.* **2013**, *85*, 2021–2026. [[CrossRef](#)]

25. Wong, A.; Boutin, C.; Aguiar, P.M.  $^1\text{H}$  high resolution magic-angle coil spinning (HR-MACS)  $\mu\text{NMR}$  metabolic profiling of whole *Saccharomyces cerevisiae* cells: A demonstrative study. *Front. Chem.* **2014**, *2*, 1–7. [[CrossRef](#)]
26. Wong, A.; Li, X.; Molin, L.; Solari, F.; Elena-Herrmann, B.; Sakellariou, D.  $\mu\text{HR-MAS}$  spinning NMR Spectroscopy for Metabolic Phenotyping of *Caenorhabditis Elegans*. *Anal. Chem.* **2014**, *86*, 6064–6070. [[CrossRef](#)] [[PubMed](#)]
27. Badilita, V.; Fassbender, B.; Kratt, K.; Wong, A.; Bonhomme, C.; Sakellariou, D.; Korvink, J.G.; Wallrabe, U. Microfabricated inserts for magic angle coil spinning (MACS) wireless NMR spectroscopy. *PLoS ONE* **2012**, *7*, e42848. [[CrossRef](#)] [[PubMed](#)]
28. Lehmann-Horn, J.A.; Jacquinet, J.F.; Ginefri, J.C.; Bonhomme, C.; Sakellariou, D. Monolithic MACS micro resonators. *J. Magn. Reson.* **2016**, *271*, 46–51. [[CrossRef](#)] [[PubMed](#)]
29. Nishiyama, Y.; Endo, Y.; Nemoto, T.; Bouzier-Sore, A.-K.; Wong, A. High-resolution NMR-based metabolic detection of microgram biopsies using a 1 mm HR $\mu\text{MAS}$  probe. *Analyst* **2015**, *140*, 8097–8100. [[CrossRef](#)] [[PubMed](#)]
30. Lucas-Torres, C.; Huber, G.; Ichikawa, A.; Nishiyama, Y.; Wong, A. HR- $\mu\text{MAS}$  NMR-Based Metabolomics: Localized Metabolic Profiling of a Garlic Clove with  $\mu\text{g}$  Tissues. *Anal. Chem.* **2018**, *90*, 13736–13743. [[CrossRef](#)] [[PubMed](#)]
31. Beckonert, O.; Keun, H.C.; Ebbels, T.M.D.; Bundy, J.; Holmes, E.; Lindon, J.C.; Nicholson, J.K. Metabolic profiling, metabolomic and metabonomic procedures for NMR spectroscopy of urine, plasma, serum and tissue extracts. *Nat. Protoc.* **2007**, *2*, 2692–2703. [[CrossRef](#)] [[PubMed](#)]
32. Kim, H.K.; Choi, Y.H.; Verpoorte, R. NMR-based metabolomic analysis of plants. *Nat. Protoc.* **2010**, *5*, 536–549. [[CrossRef](#)] [[PubMed](#)]
33. Duong, N.T.; Yamato, M.; Nakano, M.; Kume, S.; Tamura, Y.; Kataoka, Y.; Wong, A.; Nishiyama, Y. Capillary-inserted rotor design for HR $\mu\text{MAS}$  NMR-based metabolomics on mass-limited neurospheres. *Molecules* **2017**, *22*, 1289. [[CrossRef](#)] [[PubMed](#)]
34. Tate, A.R.; Foxall, P.J.D.; Holmes, E.; Moka, D.; Spraul, M.; Nicholson, J.K.; Lindon, J.C. Distinction between normal and renal cell carcinoma kidney cortical biopsy samples using pattern recognition of  $^1\text{H}$  magic angle spinning (MAS) NMR spectra. *NMR Biomed.* **2000**, *13*, 64–71. [[CrossRef](#)]
35. Cheng, L.L.; Newell, K.; Mallory, A.E.; Hyman, B.T.; Gonzalez, R.G. Quantification of neurons in Alzheimer and control brains with ex vivo high resolution magic angle spinning proton magnetic resonance spectroscopy and stereology. *Magn. Reson. Imaging* **2002**, *20*, 527–533. [[CrossRef](#)]
36. Atherton, H.J.; Bailey, N.J.; Zhang, W.; Taylor, J.; Major, H.; Shockcor, J.; Clarke, K.; Griffin, J.L. A combined  $^1\text{H}$ -NMR spectroscopy- and mass spectrometry-based metabolomic study of the PPAR- null mutant mouse defines profound systemic changes in metabolism linked to the metabolic syndrome. *Physiol. Genomics* **2006**, *27*, 178–186. [[CrossRef](#)] [[PubMed](#)]
37. Allen, N.J.; Eroglu, C. Cell Biology of Astrocyte-Synapse Interactions. *Neuron* **2017**, *96*, 697–708. [[CrossRef](#)] [[PubMed](#)]
38. Isaksson, C. Pollution and its impact on wild animals: A meta-analysis on oxidative stress. *Ecohealth* **2010**, *7*, 342–350. [[CrossRef](#)] [[PubMed](#)]
39. Derraik, J.G.B. The pollution of the marine environment by plastic debris: A review. *Mar. Pollut. Bull.* **2002**, *44*, 842–852. [[CrossRef](#)]
40. Russo, R.; Haange, S.B.; Rolle-Kampczyk, U.; von Bergen, M.; Becker, J.M.; Liess, M. Identification of pesticide exposure-induced metabolic changes in mosquito larvae. *Sci. Total Environ.* **2018**, *643*, 1533–1541. [[CrossRef](#)] [[PubMed](#)]
41. Chiu, K.H.; Dong, C.D.; Chen, C.F.; Tsai, M.L.; Ju, Y.R.; Chen, T.M.; Chen, C.W. NMR-based metabolomics for the environmental assessment of Kaohsiung Harbor sediments exemplified by a marine amphipod (*Hyaella azteca*). *Mar. Pollut. Bull.* **2017**, *124*, 714–724. [[CrossRef](#)] [[PubMed](#)]
42. Feenstra, A.D.; Alexander, L.E.; Song, Z.; Korte, A.R.; Yandean-Nelson, M.D.; Nikolau, B.J.; Lee, Y.J. Spatial Mapping and Profiling of Metabolite Distributions during Germination. *Plant Physiol.* **2017**, *174*, 2532–2548. [[CrossRef](#)]
43. Sarabia, L.D.; Boughton, B.A.; Rupasinghe, T.; van de Meene, A.M.L.; Callahan, D.L.; Hill, C.B.; Roessner, U. High-mass-resolution MALDI mass spectrometry imaging reveals detailed spatial distribution of metabolites and lipids in roots of barley seedlings in response to salinity stress. *Metabolomics* **2018**, *14*, 1–16. [[CrossRef](#)]

44. Abreu, A.C.; Aguilera-Sáez, L.M.; Peña, A.; García-Valverde, M.; Marín, P.; Valera, D.L.; Fernández, I. NMR-Based Metabolomics Approach to Study the Influence of Different Conditions of Water Irrigation and Greenhouse Ventilation on Zucchini Crops. *J. Agric. Food Chem.* **2018**, *66*, 8422–8432. [[CrossRef](#)]
45. Mucci, A.; Parenti, F.; Righi, V.; Schenetti, L. Citron and lemon under the lens of HR-MAS NMR spectroscopy. *Food Chem.* **2013**, *141*, 3167–3176. [[CrossRef](#)]
46. Pérez, E.M.S.; Iglesias, M.J.; Ortiz, F.L.; Pérez, I.S.; Galera, M.M. Study of the suitability of HRMAS NMR for metabolic profiling of tomatoes: Application to tissue differentiation and fruit ripening. *Food Chem.* **2010**, *122*, 877–887. [[CrossRef](#)]
47. Albergamo, A.; Rotondo, A.; Salvo, A.; Pellizzeri, V.; Bua, D.G.; Maggio, A.; Cicero, N.; Dugo, G. Metabolite and mineral profiling of “Violetto di Niscemi” and “Spinoso di Menfi” globe artichokes by <sup>1</sup>H-NMR and ICP-MS. *Nat. Prod. Res.* **2017**, *31*, 990–999. [[CrossRef](#)] [[PubMed](#)]
48. Kinross, J.M.; Holmes, E.; Darzi, A.W.; Nicholson, J.K. Metabolic phenotyping for monitoring surgical patients. *Lancet* **2011**, *377*, 1817–1819. [[CrossRef](#)]



© 2019 by the authors. Licensee MDPI, Basel, Switzerland. This article is an open access article distributed under the terms and conditions of the Creative Commons Attribution (CC BY) license (<http://creativecommons.org/licenses/by/4.0/>).